Computers and Geotechnics xxx (2017) xxx–xxx

Contents lists available at ScienceDirect

Computers and Geotechnics

journal homepage: www.elsevier.com/locate/compgeo

Research Paper

A numerical investigation on the yield surface for shallow foundations embedded in sand

Laura Govoni

DICAM – University of Bologna, Viale del Risorgimento 2, 40136 Bologna, Italy

ARTICLE INFO

Article history:
Received 11 April 2017
Received in revised form 21 July 2017
Accepted 25 August 2017
Available online xxxx

Keywords:
Yield surface
Embedment effects
Buried foundation
FE analyses

ABSTRACT

This paper presents a numerical study on the drained response of a shallow foundation subjected to planar combined loads. Plane strain conditions are assumed and different initial foundation depths and values of vertical penetration are considered. Data from centrifuge experiments of surface and buried foundations available in literature, are used to assess the ability of the model to reproduce the essential features of the experimentally observed behaviour. Interpreted within the context of existing work-hardening plasticity models applied to the soil-foundation system and presented in terms of load–displacement curves and load paths, the results of the numerical analyses provide new evidence of the effects of the embedment on the yield surface for a shallow foundation.

1. Introduction

It is now well established that work-hardening plasticity models [1–3] can describe accurately the plastic response of a shallow foundation under planar static combined loads (V, M, H). These models rely on the assumption that, following a given penetration, w, a yield surface develops in the load space. For a foundation of diameter D or breadth B (Fig. 1a) resting on a frictional material, the yield surface can be described by the equation [4]

$$\left(\frac{H}{V_0 h_0}\right)^2 + \left(\frac{M/B}{V_0 m_0}\right)^2 - 2a \cdot \frac{H}{V_0 h_0} \cdot \frac{M/B}{V_0 m_0} - \left[4 \cdot \frac{V}{V_0} \cdot \left(1 - \frac{V}{V_0}\right)\right]^2 = 0 \quad (1)$$

which is a cigar-shaped envelope, parabolic in sections containing the axis of vertical load (V, M/BH) and elliptical in planes at constant vertical load (H, M/B). Parameters m_0 and h_0 provide the maximum moment and horizontal dimension of the surface, while parameter a defines the rotation of its elliptical sections, as displayed in Fig. 1b. According to Eq. (1), the yield surface scales with V_0, the vertical load mobilised by the plastic component of penetration, while maintaining its shape unvaried. Single gravity and centrifuge experimental campaigns have shown that this framework essentially holds for foundations resting on the surface of homogeneous sandy samples [4–6].

The effects of the foundation embedment on the yield surface, as mobilised by the foundation penetration, w, or initial depth, d, and typically up to the foundation breadth (or diameter), have been addressed since the end of the nineties, mostly based on experimental observations.

For a shallow foundation resting on the surface of a loose sand sample, the maximum horizontal dimension of the normalised yield surface (Eq. (1)) was shown to increase linearly as a function of the sole penetration, w [7]. This trend was also observed on medium dense sand samples [8]. Results of tests on buried foundations on very dense sand showed that the size of the normalised yield surface expands following a linear trend as sole function of the initial foundation depth, d, along both the horizontal and moment dimension, with a similar rate [9]. Experiments on flat plates provided with peripheral skirts on dense sand [10], showed that the size parameters, while increasing with the skirts depth, d, also decreases as a function of V_0, reaching a minimum at the maximum allowable vertical load, V_{peak}. A significant influence of the effects of the skirts on the yield surface rotation (parameter a) was also observed in the study. An increase in the normalised yield surface size and rotation due to the presence of skirts about the foundation perimeter was also observed in loose sand [11]. These tests also showed that, in presence of very low values of vertical load, the normalised yield surface might extend in the tensile range of vertical load, a tendency also observed more recently on dense sand [12]. Results of centrifuge tests on buried foundations in sand samples of medium density displayed a normalised yield surface function of the foundation initial depth, d, and penetration,

E-mail address: l.govoni@unibo.it

http://dx.doi.org/10.1016/j.compgeo.2017.08.017
0266-352X/

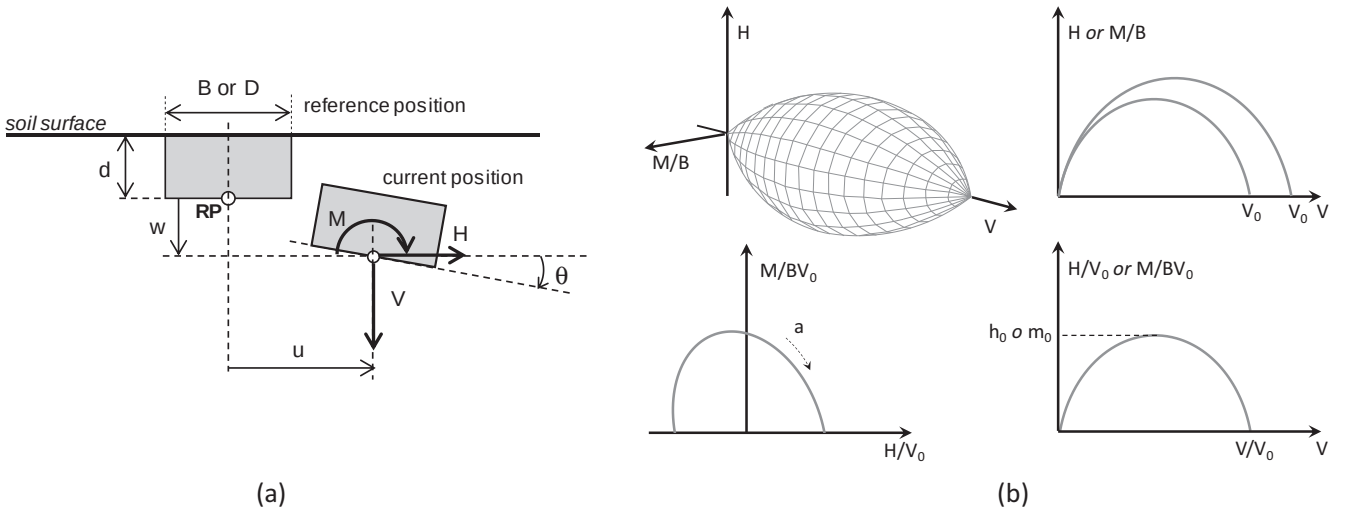

Fig. 1. Combined loading capacity of a shallow foundation: (a) problem position and (b) schematic representation of the yield surface after [24,27].

w [13]. In the tests, a rather large normalised yield surface, established at low values of penetration (w/D < 0.05), was observed to quickly reduce as the penetration increased (up to w/D ~ 0.1) to resume its expansion at higher penetrations (w/D > 0.1). This trend was attributed to a response dominated by the soil dilatancy at low confining stresses and by the foundation embedment at comparatively larger values of penetration. As the experimental apparatus enabled to explore only a small portion of the yield surface, these effects could not be quantified, although a consistent and clear trend was envisaged.

At present, a general expression for the yield surface for a buried foundation, which takes into account the initial depth and the foundation penetration, which is not related to the definition of V_{peak}, is notably absent. This provides the motivation of this study which aims at exploring the yield surface for a shallow foundation, across a practical range of depth and penetration values, using a simple numerical model, suitably developed and validated based on experimental data available in literature [13].

The use of numerical models to investigate the undrained combined bearing capacity of surface embedded foundations dates back to the end of the nineties [14] and is now well consolidated [15–17]. Besides, numerical investigation on the drained combined capacity of an embedded foundation are more recent and relevant to specific cases of study, such as mono-caisson for offshore wind turbines [18] or bridge piers (d/D > 1) [19]. Within the context of work-hardening plasticity models, numerical investigation have concerned so far analyses of strip surface and buried foundations under pure eccentric and pure inclined loads [20–22]. However, in these preliminary studies, the ability of the model in capturing the essential features of the foundation behaviour was not assessed by comparison with experimental observations. A numerical work, which proved the ability of a simple finite element (FE) model to capture some aspects of the experimentally observed behaviour of a buried foundation was presented in [23] and provides the starting point of this study. In this study, the validation of this FE model is extended further in presence of various load paths, M/BH, depths of initial burial, d/B, and vertical load mobilisation, V_0. The FE model is then used to explore the effects of the embedment on the yield surface of a buried foundation. Three depths of initial burial (d/B = 0, 0.5, 1), two values of penetration (w/B = 0.1, 0.2) along several load paths are considered, for surface and buried foundations which fail according to a punching-shear mode under pure vertical load. The applicability of Eq. (1) to the numerical results is thus assessed and the size and rotation parameters are calibrated and expressed as function of d and w. Results find application across a wide range of case in which a buried foundation is subjected to general loading conditions [24–26].

2. Details of the numerical study

Two-dimensional, large-strain finite element analyses (FEA) were carried out to model the long-term, planar combined loading response of a shallow foundation. To the scope, the commercial software Abaqus was used [28]. The effectiveness of the modelling choices, which moved from those introduced and discussed in the work presented in [23], were validated based on selected results of a set of centrifuge tests of buried footings on medium dense silica sand samples. These tests, all presented and interpreted in a recent publication [13], provided the experimental reference for the numerical study.

2.1. Soil and foundation properties

The foundations were of breadth B, initial depth d/B = 0, 0.5 and 1 and modelled as solid rigid bodies. The interface between the foundations and the soil was prescribed as fully rough in shear. As depicted in Fig. 2, the mesh boundaries were placed at a distance of 5B from either side of the foundation and 5B from the soil surface. The soil was discretised by four node, bi-linear, plane strain, reduced integration, continuum elements (CPE4R) and modelled as an elasto-plastic material yielding according to the Mohr Coloumb failure criterion. Four nodes elements were used, as convergence issues were observed due to strong mesh deformations, using more accurate eight nodes elements in combination with large-strain analyses [28]. Previous numerical studies, which has considered shallow foundations on a Mohr Coulomb material, have shown the approach to be effective for general loading problems of a foundation, yielding results consistent with experimental data [18,23] or in agreement with more sophisticated constitutive models [19]. Plane strain conditions were considered for simplicity, as the foundation shape was shown to have negligible effects in presence of planar combined loading conditions [9]. Elasto-plastic model parameters (E = 40 MPa, ν = 0.3, ϕ' = 30°, ψ = 5°, γ' = 10 kN/m^3, c′ = 1 kPa) were selected to provide an overall satisfactory agreement to the centrifuge data. Although with a slightly lower value ψ, the parameters were also shown to essentially fit the results of drained triaxial compression tests (R_D = 40.5%, p'_0 = 50, 300 kPa), carried out on the silica sand used in the experiments, as shown in Fig. 3, where the elastic modulus was E = 25, 45 MPa for p'_0 = 50, 300 kPa respectively.

Please cite this article in press as: Govoni L. A numerical investigation on the yield surface for shallow foundations embedded in sand. Comput Geotech (2017), http://dx.doi.org/10.1016/j.compgeo.2017.08.017

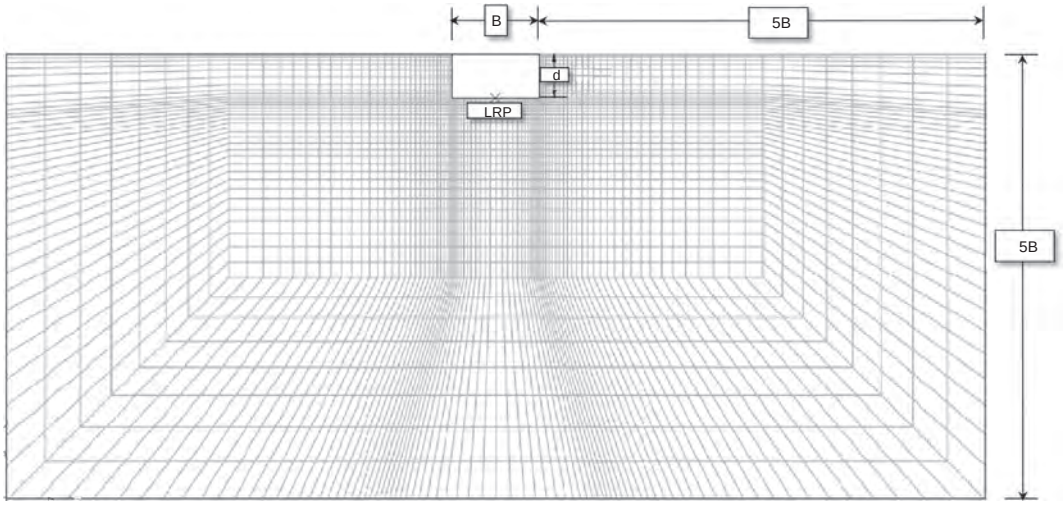

Fig. 2. Finite element mesh.

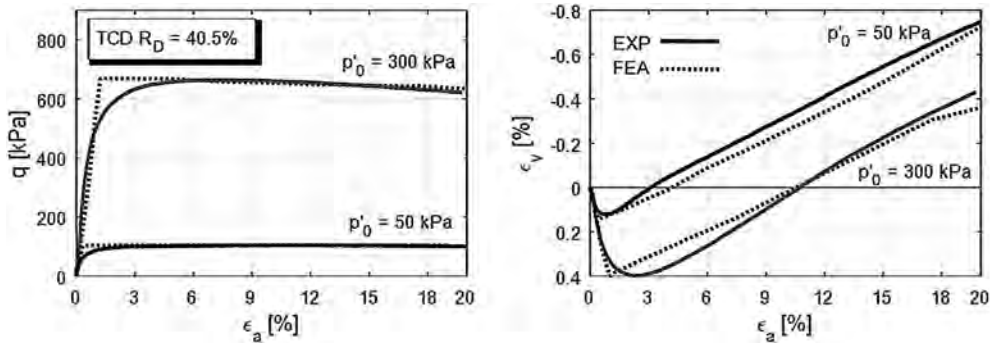

Fig. 3. FE modelling of two drained compression triaxial tests on samples of silica sand.

2.2. Details on the numerical analyses

The foundation models were subjected to pure vertical, V, and planar combined loading tests. All tests were displacement controlled and carried out in large-strain in order to reproduce the embedment-dependent increase in the foundation bearing response. All foundation models (d/B = 0, 0.5 and 1) were subjected to vertical load tests to describe the foundation vertical load - vertical displacement curve up to a penetration ratio, w/B, equal to 0.2. In-plane combined load tests were all of the swipe type. A swipe test allows the yield surface corresponding to a given vertical penetration of the foundation to be identified in a single experiment [4]. A vertical displacement is applied to the foundation to set up the reference plastic displacement and the corresponding reference vertical load, V_0. The vertical displacement is then held constant while the footing is driven along a rotational or horizontal displacement path, θB/u, in a 'swipe event'. Swipe tests were also carried out in which the foundation was first displaced vertically to a given depth to set up the reference vertical load, V_0, and then unloaded to a proportion of the reference vertical load, V/V_0 before a swipe event was carried out. So far, numerical swipe tests have considered only pure horizontal and rotational (θB/u = 0, ∞) paths [20–23]. In this study, numerical swipe tests have been also performed along various rotational to horizontal displacement paths, θB/u, from different values V_0. Along with the embedment details (d/B, w/B), Table 1 provides the value of initial vertical effective stress at a depth equal to B/2 below the foundation, $\sigma'_{v0} = \gamma'(B/2 + d)$, the dimensionless reference vertical load, $V_0/B\ \sigma'_{v0}$, and the dimensionless vertical load, $V/B\ \sigma'_{v0}$, at which the swipe event was carried out, and assigned displacement path, θB/u. Reference centrifuge tests used for the model validation are also identified and labelled in the farthest right column of Table 1.

Eight different centrifuge swipe tests were selected with the scope of validating the numerical model. The tests were all carried out at 100*g* in the UWA drum centrifuge. A superfine silica sand sample was prepared by dry pluviation prior to be saturated. The sample uniformity and relative density (50 ∼ %, $\gamma' \sim 10$ kN/m^3) were assessed by interpreting the results of a set of miniature cone tests. Two different foundation diameters were considered in the centrifuge study D = 50 mm and D = 30 mm, which corresponded at 100*g* to prototype diameters of 5 m and 3 m. The loading test were all carried out to ensure the results were not affected by the boundary conditions. Further experimental details are found in [13]. The list of experiments used for the purpose of model calibration is provided in Table 2, where the reference numerical tests of Table 1, are associated to the corresponding experiments. Reference numerical tests involved a 3 m and 5 m foundation breadth as in the corresponding experiments. Experiments concerned 3 initial foundation depths, values of $V_0/A\ \sigma'_{v0}$ ranging between 20 and 40 and essentially 3 load paths, ranging between pure moment loading condition to M/DH ∼ 1.

3. Results of the numerical analyses

Results of the numerical analyses are presented in terms of displacement - load curves and load paths in a dimensionless form. In particular, loads are divided by the foundation breadth and initial

Please cite this article in press as: Govoni L. A numerical investigation on the yield surface for shallow foundations embedded in sand. Comput Geotech (2017), http://dx.doi.org/10.1016/j.compgeo.2017.08.017

Table 1
Details of the numerical swipe tests.

d/B	σ'_{v0} [kPa]	w/B	$V_0/B\ \sigma'_{v0}$	$V/B\ \sigma'_{v0}$	R = θB/u	Reference test name
0	25	0.1	22.5	22.5	4	SW1R4
					0, ±0.5, ±1, ±2, −4, ∞	
				1.4	0, ∞	
		0.2	26.6	26.6	0, +1, ±2.5, ±4	
					∞	SW2 M
				0.9	0	
					∞	$SW1M_{low}$
0.5	50	0.1	21.4	21.4	0, ±0.5, ±1, ±2, ±4, ∞	
				2.1	0, ∞	
		0.2	32.5	32.5	2.5, ∞	B1W2R25, B1W2M
					±1, −2.5, ±4	
				1.7	0	
					∞	$B1W2M_{low}$
1	75	0.1	19.4	19.4	0, ±1, ±2.5, ±4, ∞	
				1.7	0, ∞	
		0.2	27.4	27.4	4	B2W2R4
					0, ±1, ±2.5, −4, ∞	
				0.9	0	
					∞	$B2W2M_{low}$

Table 2
Details of centrifuge data [13] selected for the numerical model validation.

Centrifuge test	D [m]	d/D	$V_0/A\ \sigma'_{v0}$	$V/A\ \sigma'_{v0}$	Load path	FE test
LGS06	5	0	20.3	20.3	H ~ 0	SW2M
LGS07	5		30.8	30.8	High M/DH	SW1R4
LGS11	5		34.5	3.2, after unloading	H ~ 0	$SW2M_{low}$
LGB05	5	0.5	42.2	42.2	High M/DH	B1W2R4
LGB16	5		38.7	38.7	M/DH ~ 1	B1W2R25
LGB11	5		30.9	7, after unloading	H ~ 0	$B1W2M_{low}$
LGB19	3	1	30.1	30.1	High M/DH	B2W2R4
LGB12	3		0.09	29.6	H ~ 0	$B2W2M_{low}$

stress level, $B\ \sigma'_{v0}$, as in [13] and according to Table 1. Swipe paths are also normalised by the reference vertical load, V_0, facilitating comparison with the cigar-shaped yield surface as described by Eq. (1). In such normalisation, data were corrected for the soil elasticity, following the procedure illustrated in [20]. First, the consistency of the modelling choices and modelling parameters are assessed by comparing the results of the numerical analyses with the centrifuge data according to Table 2. Then, the applicability of Eq. (1) to the numerical results is verified and the relevant model parameters are given.

3.1. Vertical loading response

In Fig. 4, the numerical response of the three foundation models (d/B = 0, 0.5, 1) to pure vertical load is shown. The bearing pressure, V/B, increases with w/B, as typical of the punching behaviour expected for a shallow foundation embedded in a medium dense sand bed (Fig. 3a). Division of the vertical loads by $B\ \sigma'_{v0}$, results in a consistent response of the three curves as shown in Fig. 3b, suggesting that the bearing capacity of the foundation models increases almost linearly with the depth of initial burial, d. The numerical results can be described, as proposed in [5] by the functional form

$$\frac{V}{B\cdot\sigma'_v}=\left(\frac{k_1}{\sigma'_{v0}}\right)\cdot\frac{w_p}{B}\cdot\left[\frac{1+\left(\frac{B}{w_1}\right)\cdot\frac{w_p}{B}}{1+\left(\frac{B}{w_2}\right)\cdot\frac{w_p}{B}}\right]$$

$$\frac{w_p}{B}=\frac{w}{B}-\frac{V}{B\cdot\sigma'_v}\left(\frac{\sigma'_v}{K_e}\right) \qquad (2)$$

where w_p is the plastic component of the foundation penetration and $k_1/\sigma'_{v0} = 1236$, $B/w_1 = 0.365$, $B/w_2 = 0.0184$, $K_e/\sigma'_{v0} = 660$ are the best-fit dimensionless parameters. Eq. (5), calibrated based on the vertical load centrifuge data, is also inserted in Fig. 4b (with average $K_e/\sigma'_{v0} = 3500$). The curves show a similar trend, although the centrifuge foundation models exhibit a consistently higher capacity with penetration. Solution of the problem through the method of stress characteristic is also displayed in Fig. 4b and calculation was as follows. The vertical bearing capacity was evaluated using the slip line method, through the free software ABC [29], assuming the foundation penetration, w, as an additional surcharge $q'_0 = \gamma'(d + wB)$, for each strip foundation with parameters, $\phi' = 30°$, $\gamma' = 10\ kN/m^3$, d/B = 0, 0.5, 1. The resulting three curves were then interpolated with the best-fit straight line, showing a good agreement with the FE response.

3.2. Combined loading response

With reference to the surface foundation (d/B = 0) and according to Table 2, Fig. 5 shows the results of three numerical swipe tests and corresponding centrifuge data. In particular, the data from tests carried out from the lower value of $V_0/B\ \sigma'_{v0}$ (~20) along a dominant moment path are given in Fig. 5a and b. Both the moment and smaller horizontal components of load are shown, in terms of load - displacement curve (Fig. 4a) and load paths (Fig. 5b). Results of tests carried out from $V_0/B\ \sigma'_{v0} \sim 30$ along a pure moment path, directly or following unloading, are instead shown in Fig. 5c-d. Consistency is observed between the numerical and experimental data along the load-displacement curves while the load paths tracked by the virtual foundations also closely track the experimental, following an essentially parabolic shape. The agreement in the response in terms of load paths becomes clearer when loads are normalised by V_0, as displayed in Fig. 5e-f, where

Please cite this article in press as: Govoni L. A numerical investigation on the yield surface for shallow foundations embedded in sand. Comput Geotech (2017), http://dx.doi.org/10.1016/j.compgeo.2017.08.017

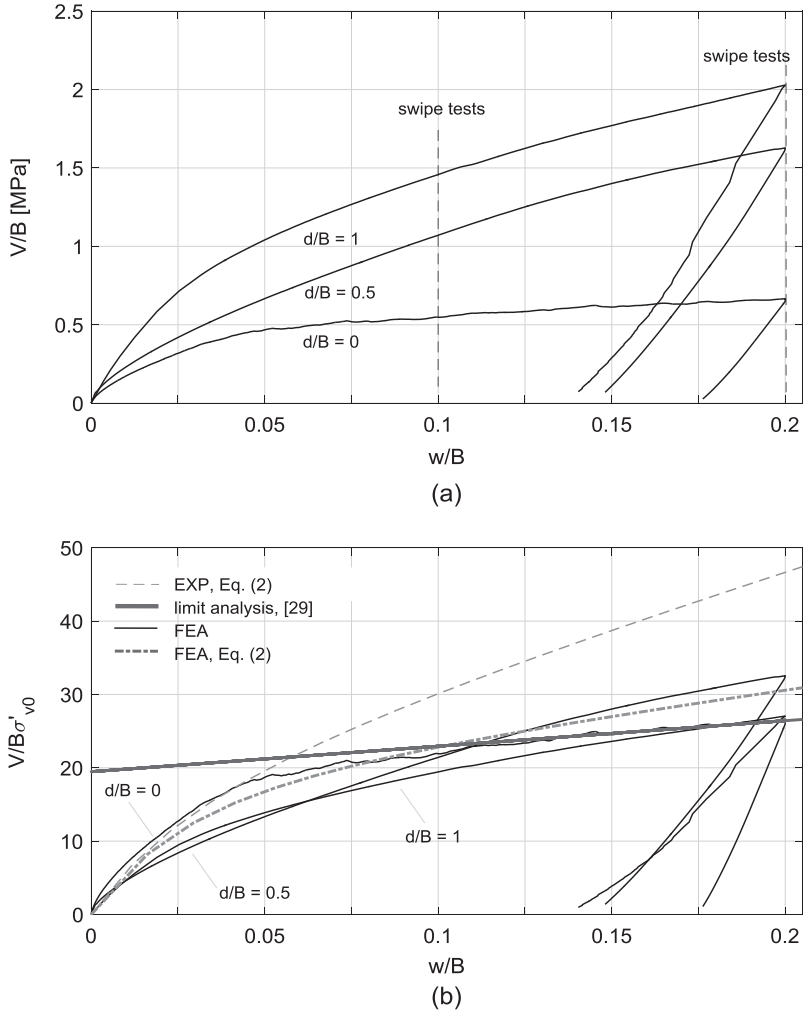

Fig. 4. Numerical vertical loading tests on surface and buried footings (a) penetration ratio against vertical pressure and (b) penetration ratio against dimensionless vertical load.

the three couples of tests are displayed. The normalisation enables to eliminate the scatters ascribable to a slight diverse $V_0/B\ \sigma'_{v0}$, in the corresponding numerical and experimental swipe events. The results of four numerical swipes performed on the two buried foundation models featuring d/B = 0.5 and d/B = 1 are shown, along with the corresponding data obtained in the centrifuge tests (Table 2), in terms of dimensionless load-displacement response and swipe paths in Figs. 6 and 7 respectively. As for the shallower buried foundation (d/B = 0.5), $V_0/B\ \sigma'_{v0}$ was about 30 for all the tests and three different load paths were considered. Results of a swipe event carried out at a high M/BH ratio is inserted in Fig. 6a and b where both the moment and horizontal component of load are shown along with data of a pure moment swipe following unload. The horizontal and moment component of load of a tests featuring a M/BH ratio approximately equal to 1 are inserted in Fig. 6c-d and Fig. 6e-f, respectively. Comparison between the numerical and experimental data shows that a good agreement exists between the two, along the hardening type load - displacement curve and the circa parabolic swipe paths. The load paths are normalised by V_0, in Fig. 8a-c to enable a quantitative comparison. Eq. (2) was used here to provide the actual V_0, in the normalisation of the swipe paths according to [20]. As observed, the numerical normalised swipe paths approximates closely the corresponding experimental curve, although a slightly greater moment capacity is shown for the tests at the high M/BH ratio (Fig. 8c). The two numerical swipes on the foundation model with d/B = 1 (Figs. 7 and 8d) were carried out from $V_0/B\ \sigma'_{v0} \sim 25$ along a high M/BH ratio path and a pure moment path, following unloading. In presence of a higher initial depth the experimental load –displacement response become stiffer and the load path steeper, a trend that the numerical model seems able to capture as observed by comparison of numerical swipe B1W2R4 and centrifuge swipe B19 (Fig. 7). The load paths normalised by V_0, shows that the numerical buried foundation mobilises a moment capacity slightly higher than the centrifuge foundation as yet observed for the shallower foundation model (d/B = 0.5, Fig. 8c).

Overall, the numerical models of surface and buried foundations were shown able to reproduce the essential features of the combined loading response observed on centrifuge model tests in presence of relatively high values of reference vertical load ($V_0/B\ \sigma'_{v0} > 20$) and along different load paths.

3.3. Interpretation of the results in terms of yield surface

The load paths tracked by the foundation in all the swipe events (Table 1) were normalised by V_0 to enable the result of the numerical analyses to be compared to Eq. (1). Once parameters h_0, m_0 ad *a* had been suitably calibrated, by defining the quantity [4]

Please cite this article in press as: Govoni L. A numerical investigation on the yield surface for shallow foundations embedded in sand. Comput Geotech (2017), http://dx.doi.org/10.1016/j.compgeo.2017.08.017

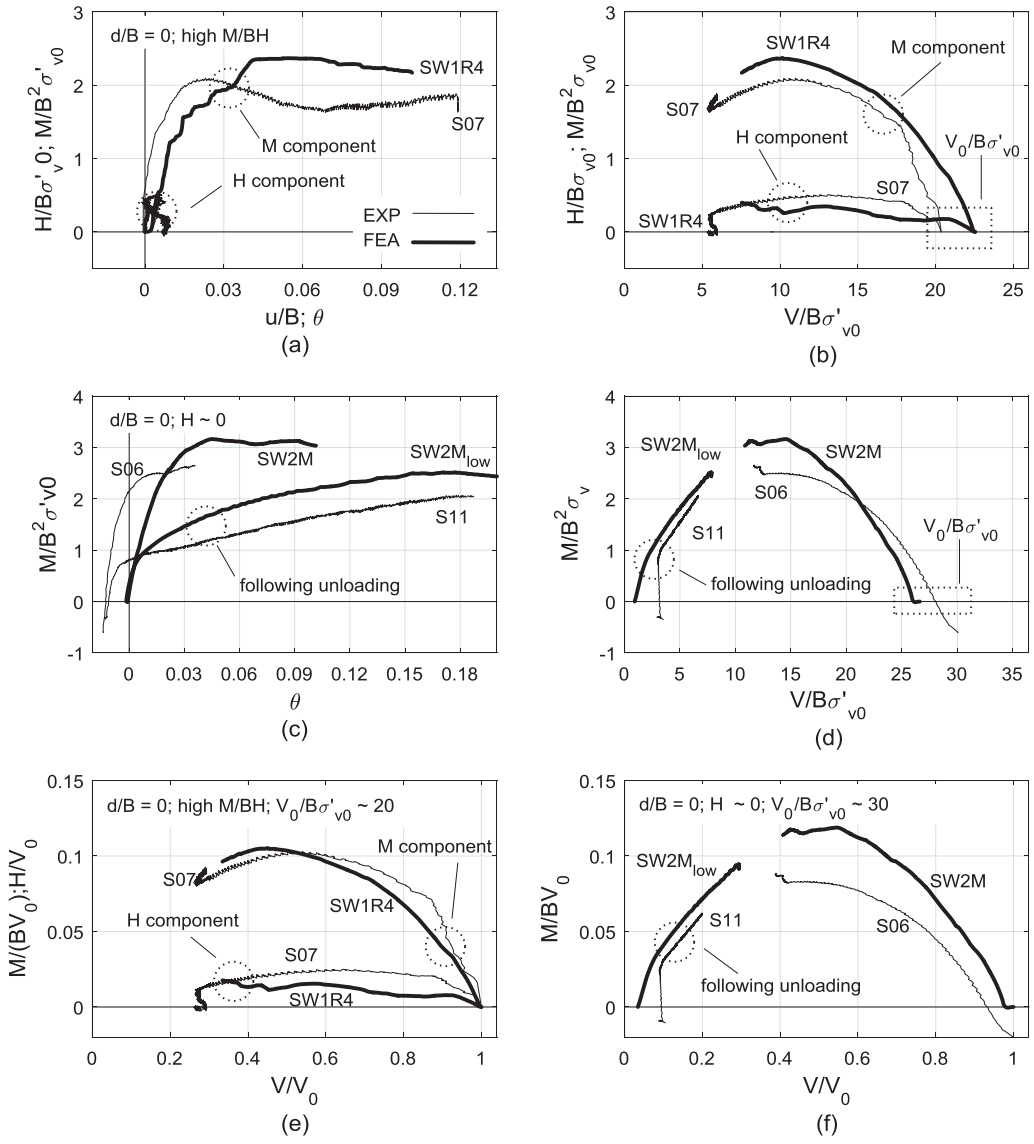

Fig. 5. Results of the numerical swipe tests on the surface foundation (d/B = 0) and comparison with the relevant centrifuge data in terms of (a and c) dimensionless combined load-displacement curves; (b and d) dimensionless load paths; (e and f) load paths normalised by V_0.

$$\frac{Q}{V_0} = \sqrt{\left(\frac{H}{V_0 h_0}\right)^2 + \left(\frac{M/B}{V_0 m_0}\right)^2 - 2a \cdot \frac{H}{V_0 h_0} \cdot \frac{M/B}{V_0 m_0}} \quad (3)$$

it was possible to reduce all the data to fit a weighted parabola on the normalised deviatoric plane (Q/BV_0, V/V_0), so that the consistency of the data to Eq. (1) could be clearly be observed.

Eq. (1) proved suitable to interpolate the normalised load paths of the 21 numerical swipe tests carried out on the surface foundation model (d/B = 0, Table 1). As the effect of the penetration, w, on the normalised yield surface revealed not negligible, two set of parameters were needed to successfully interpolate the numerical observations. The best - fit parameters, calculated through a least square regression were: $h_0 = 0.1132$, $m_0 = 0.1033$ and $a = -0.0178$, for $w/B = 0.1$ and $h_0 = 0.1279$, $m_0 = 0.1150$ and $a = -0.3026$ for $w/B = 0.2$. Normalised load paths are shown in Fig. 9 on the (M/BV_0, H/V_0) plane (Fig. 9a-c) highlighting with markers the data points corresponding to $V/V_0 = 0.5$, 0.6. Slices of the Eq. (1), plotted with the relevant parameters, at $V/V_0 = 0.5$, 0.6 are also inserted in Fig. 9a-c. The quality of the fit can be appreciated on Fig. 9b-d, on the deviatoric plane (Q/BV_0, V/V_0) were data, processed according to Eq. (6), are shown to fall in relatively narrow band about Eq. (1).

Eq. (1) also applied to describe the load paths tracked by the buried foundation model of d/B = 0.5. Best-fit parameters were: $h_0 = 0.1265$, $m_0 = 0.1019$ and $a = -0.1222$, for values of vertical penetration $w/B = 0.1$ and $h_0 = 0.2145$, $m_0 = 0.1592$ and $a = -0.1326$ for values of vertical penetration $w/B = 0.2$. As for the surface footing, the foundation penetration influenced both the extent and rotation of the normalised yield surface and two different sets of parameters were needed to successfully interpolate the numerical data. The load paths of the 22 numerical swipe tests, divided by V_0, inserted in normalised (M/BV_0, H/V_0) plane along with slices of the Eq. (1) at values of $V/V_0 = 0.6$ in Fig. 10a-b and in the deviatoric plane (Q/BV_0, V/V_0) in Fig. 10b-d show consistency with Eq. (1).

The increase in the foundation initial penetration (d/B = 1) affected the size of normalised yield surface, but a deviation from Eq. (1) was also observed on the shape, as it was also observed in the centrifuge experiments (e.g. Fig. 8d). Nonetheless, best-fit parameters could be determined: $h_0 = 0.2328$, $m_0 = 0.2280$ and $a = -0.6289$, for $w/B = 0.1$ and $h_0 = 0.2988$, $m_0 = 0.2116$ and

Please cite this article in press as: Govoni L. A numerical investigation on the yield surface for shallow foundations embedded in sand. Comput Geotech (2017), http://dx.doi.org/10.1016/j.compgeo.2017.08.017

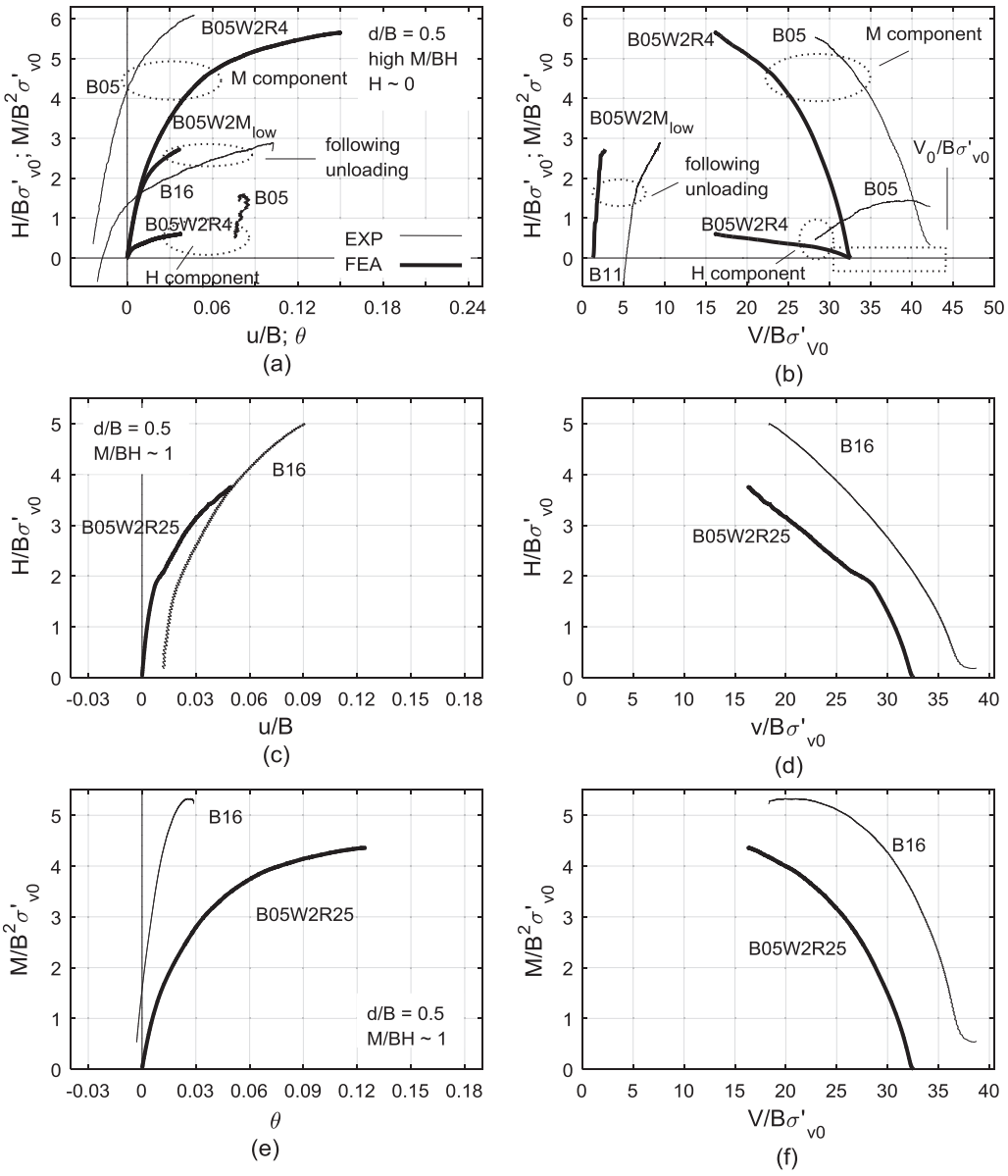

Fig. 6. Results of the numerical swipe tests on buried foundations (d/B = 0.5) and comparison with the relevant centrifuge data in terms of (a), (c) and (e) dimensionless combined load-displacement curves; (b), (d) and (f) dimensionless load paths.

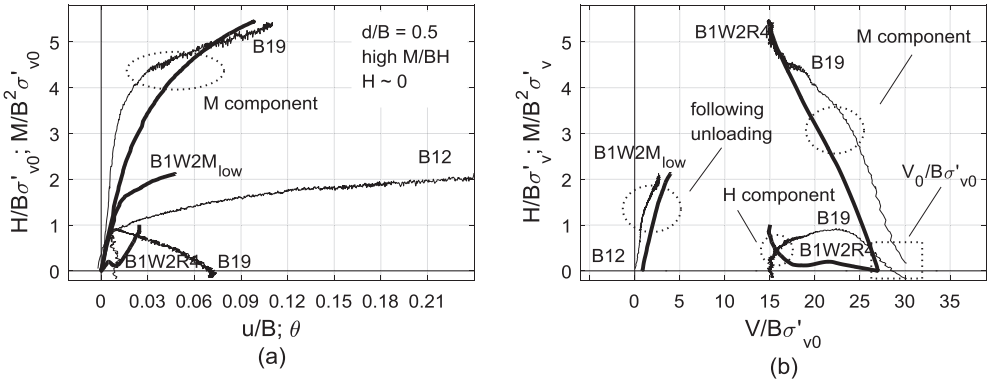

Fig. 7. Results of the numerical swipe tests on buried foundations (d/B = 1) and comparison with the relevant centrifuge data in terms of (a) dimensionless combined load-displacement curves (b) dimensionless load paths.

Please cite this article in press as: Govoni L. A numerical investigation on the yield surface for shallow foundations embedded in sand. Comput Geotech (2017), http://dx.doi.org/10.1016/j.compgeo.2017.08.017

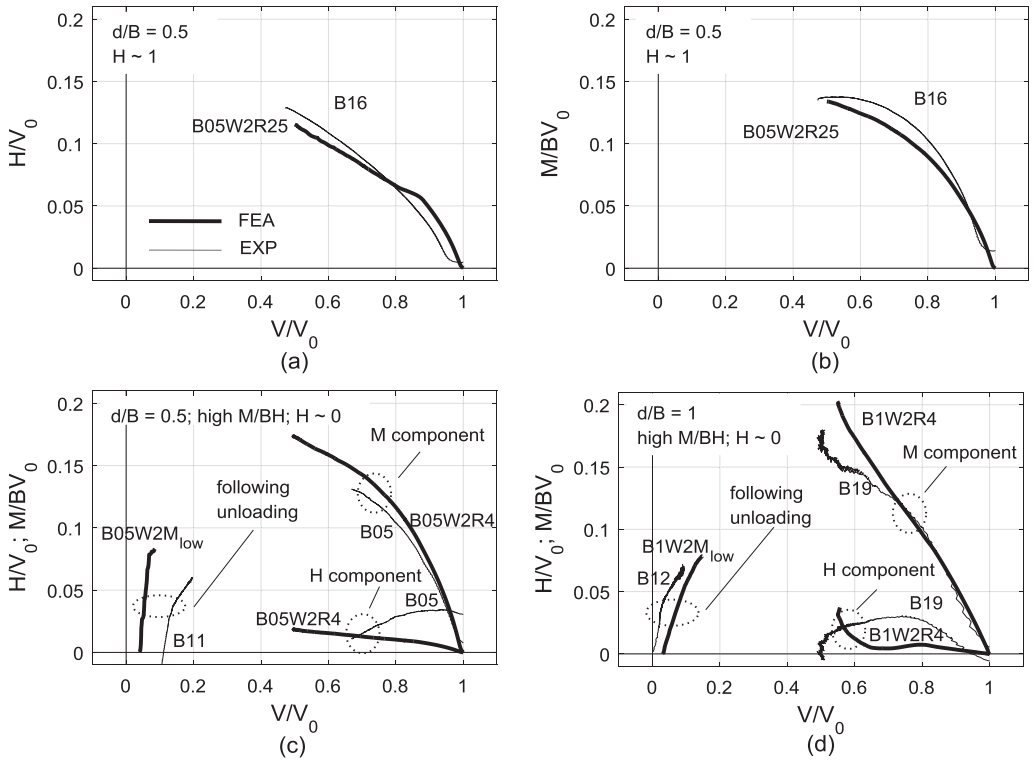

Fig. 8. Results of the numerical swipe tests on buried foundations and comparison with the relevant centrifuge data in terms of load paths normalised by V_0: (a), (b) and (c) d/B = 0.5 and (d) d/B = 1.

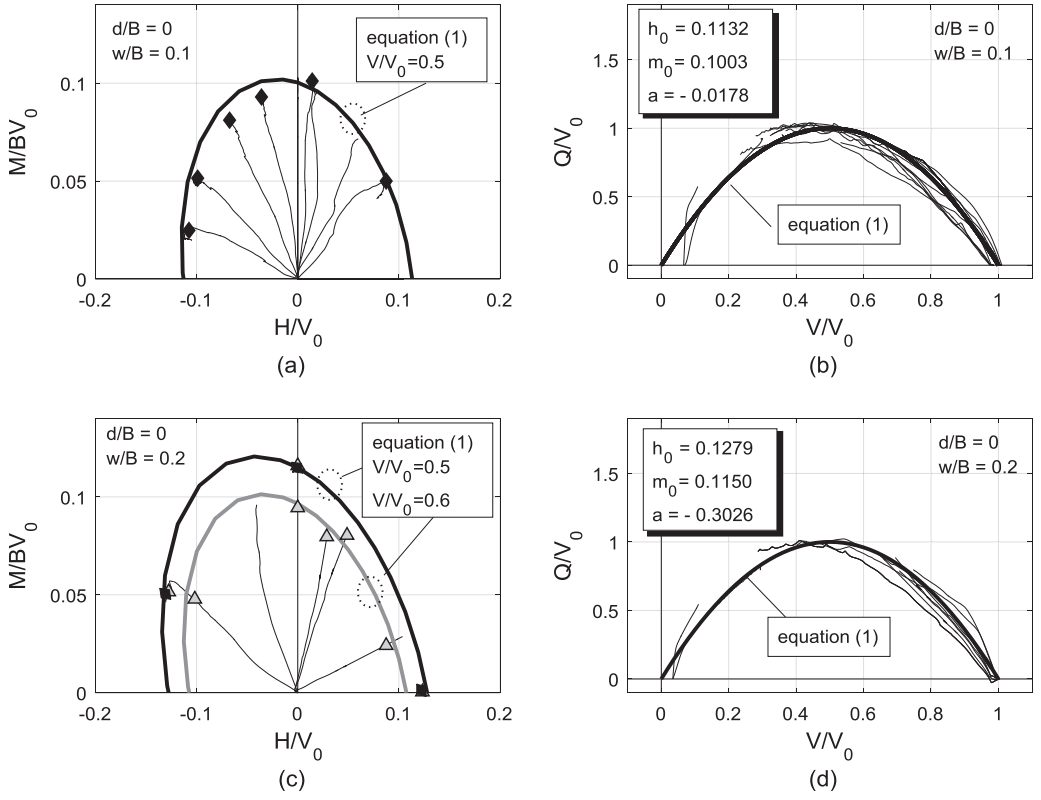

Fig. 9. Normalised load paths of surface foundations (d/B = 0), (a) and (c) on plane (M/BV_0, H/V_0); (b) and (d), on the deviatoric plane.

Please cite this article in press as: Govoni L. A numerical investigation on the yield surface for shallow foundations embedded in sand. Comput Geotech (2017), http://dx.doi.org/10.1016/j.compgeo.2017.08.017

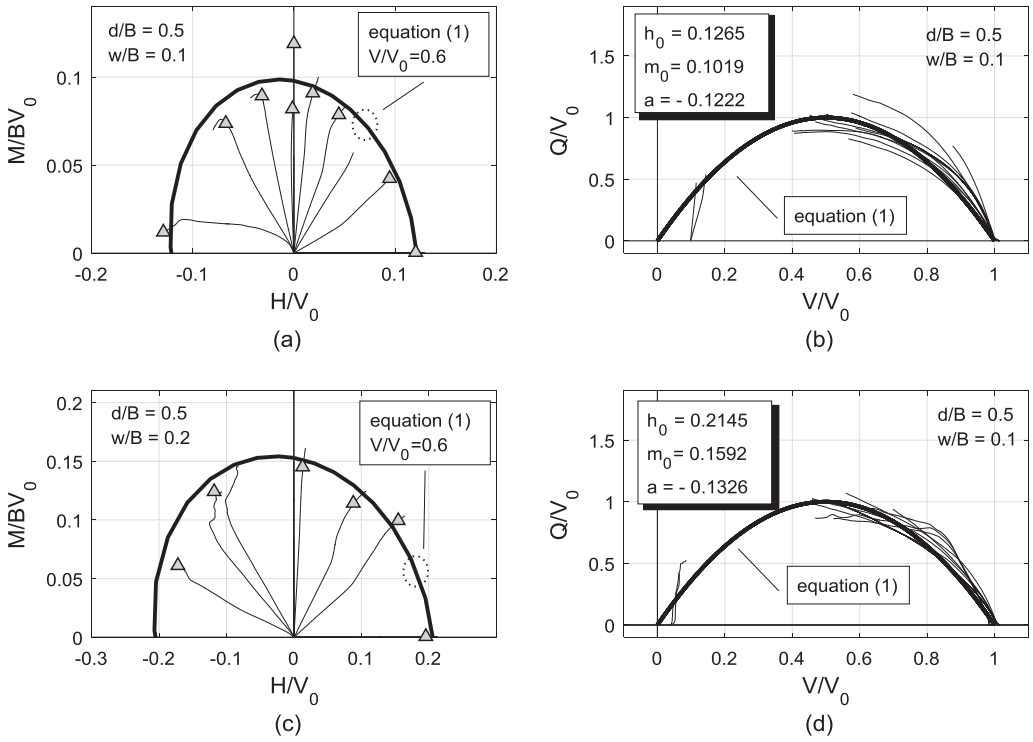

Fig. 10. Normalised load paths of buried foundations (d/B = 0.5), (a) and (c) on plane (M/BV_0, H/V_0); (b) and (d), on the deviatoric plane.

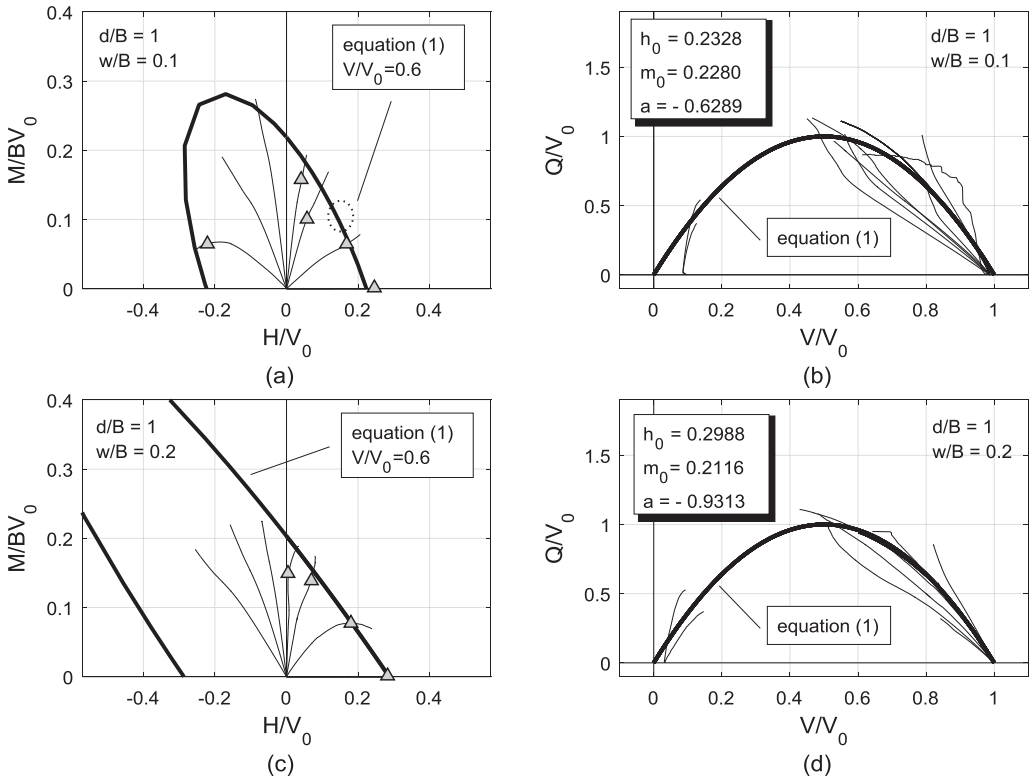

Fig. 11. Numerical results of swipe tests on buried foundations (d/B = 1), (a) and (c) load paths on the (M/BV_0, H/V_0) plane, (b) and (d) load paths on the (Q/BV_0, V/V_0) plane.

a = −0.9313 for w/B = 0.2. Normalised data are given in Fig. 11, on the (M/BV_0, H/V_0) plane (Fig. 11a and b) and on the deviatoric plane (Q/BV_0, V/V_0) (Fig. 11(b) and (d)), where the effect of the foundation depth on the shape of the surface can be appreciated when swipe paths are compared with the parabolic shape of Eq. (1).

Fig. 12 shows the evolution of the yield surface size and (h_0, m_0) and rotation (a) parameters with the foundation embedment, as

Please cite this article in press as: Govoni L. A numerical investigation on the yield surface for shallow foundations embedded in sand. Comput Geotech (2017), http://dx.doi.org/10.1016/j.compgeo.2017.08.017

observed in the FE analyses and mobilised by both the foundation initial depth, d, and vertical penetration, w. In Fig. 12, results of previous experimental observations are also inserted.

In particular, data relevant to sole effect of the foundation penetration, w, described by equation

$$h_0 = 0.138 + 0.093 \cdot \frac{w}{D} \quad (4)$$

as obtained from circular surface foundations (d/D = 0) on loose sand are considered for comparison [7]. The contribution of the foundation initial depth, d, as observed on square buried foundations ($w \sim 0$, $V_0 = 0.06V_{peak}$, d/D = 0, 0.1, 0.25, 0.5) on very dense sand is represented in Fig. 12, through the equations [9]

$$m_0 = 0.0875 + 0.075 \cdot \frac{d}{B}$$
$$h_0 = 0.12 + 0.18 \cdot \frac{d}{B} \quad (5)$$

Fig. 12 also displays the results of tests on skirted foundation on dense sand at $V_0 = V_{peak}$ [10] and data of skirted foundation on loose sand obtained at low values of vertical load mobilisation V_0 [11]. The relevant values are given in Table 3.

In Fig. 12a and b, the effects of the embedment on size of the normalised yield surface (m_0, h_0) are displayed. Results of the numerical study showed that an essentially linear trend exists between the maximum moment and horizontal dimension of the surface and the foundation embedment, owing to both the initial foundation depth and penetration (d + w), described by the following expression

$$m_0 = 0.0872 + 0.151 \cdot \frac{d+w}{B}$$
$$h_0 = 0.791 + 0.131 \cdot \frac{d+w}{B} \quad (6)$$

The trend observed in this numerical study, is consistent with data of previous experimental works. Results of the study shows that, for a buried foundation, the size of the normalised yield surface increases as function of both the initial depth, d, and the foundation penetration, w, which contribute to the mobilisation of the embedment, suggesting that the two quantities should be incorporated into Eq. (1) through Eq. (6). Fig. 12c shows the variation of parameter *a*, which governs the rotation of the yield surface in its elliptical sections. Although with no clear trend, data show a

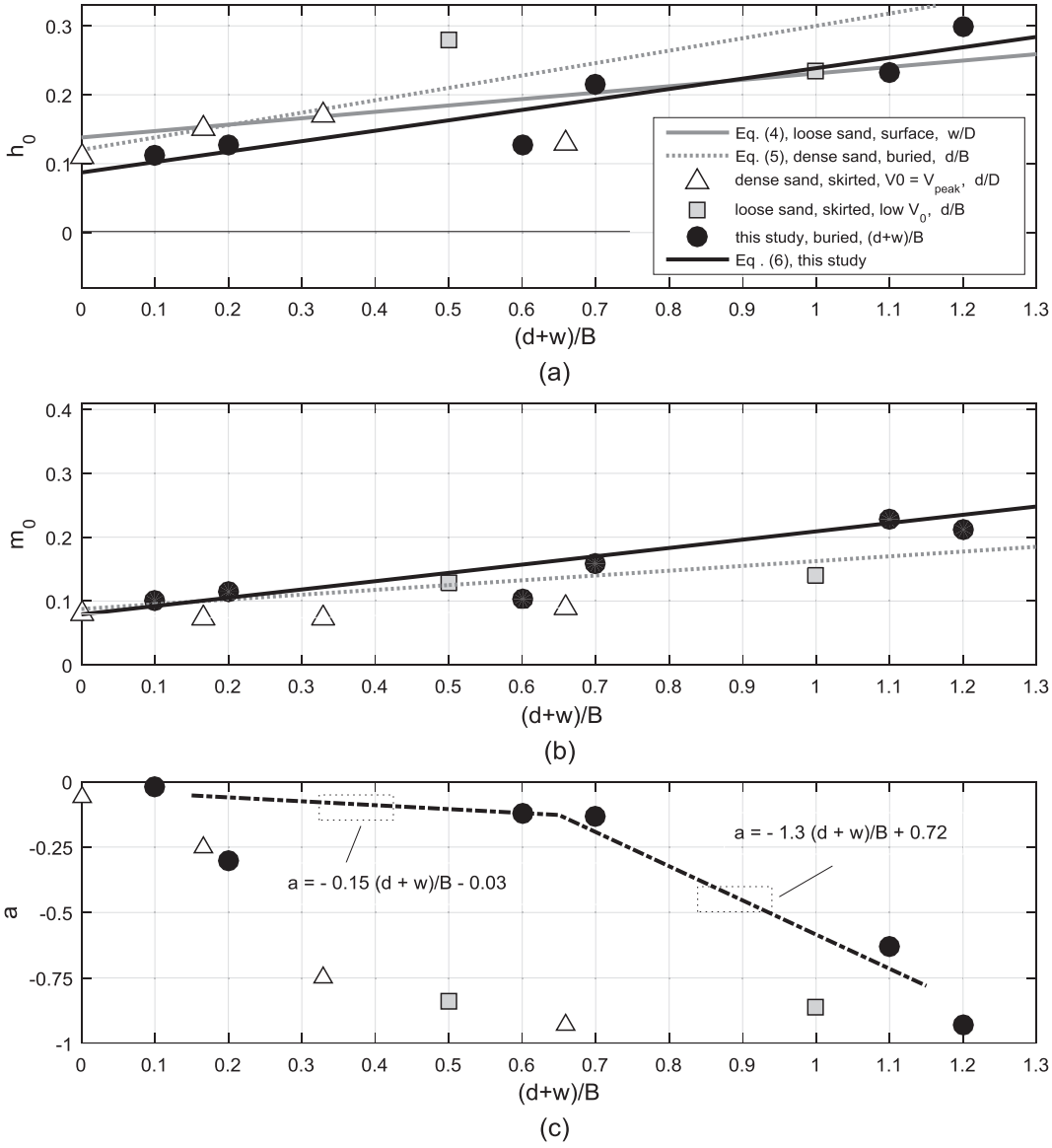

Fig. 12. Effects of the embedment depth on the normalised yield surface, as observed in the FE analyses compared with previous studies, in terms of: (a) horizontal dimension, h_0, (b) moment dimension, m_0 and (c) rotation of the elliptical sections, *a*.

Please cite this article in press as: Govoni L. A numerical investigation on the yield surface for shallow foundations embedded in sand. Comput Geotech (2017), http://dx.doi.org/10.1016/j.compgeo.2017.08.017

Table 3
Yield surface parameters for skirted foundations in sand [10,11].

Ref.	R_D	V_0	d/D	m_0	h_0	a
[10]	Dense	High, V_{peak}	0	0.08	0.11	−0.06
			0.16	0.074	0.15	−0.25
			0.33	0.074	0.17	−0.75
			0.66	0.09	0.13	−0.93
[11]	Loose	Very low	0.5	0.128	0.279	−0.84
			1	0.124	0.235	−0.86

decrease of the parameter with the embedment, corresponding to a significant increase in the anticlockwise rotation of the yield surface. A similar tendency was also observed on skirted foundations on dense and loose sand as illustrate in Fig. 12c, although with a scatter for values of embedment depths of about half diameter. A schematic fitting of the data is also inserted in Fig. 12c, which can be used to include the embedment effects on the yield surface rotation in Eq. (1).

4. Discussion

The results of the study have shown that a linear-elastic perfectly plastic constitutive model, can give a rather accurate picture of the soil-foundation plastic response under planar combined loading, for a shallow foundation embedded in a uniform, medium dense, sand bed. The data obtained from the study, suitably interpreted, find applications over a practical range of initial foundation depth and vertical load mobilisation values.

Accounting for the embedment effects on the yield surface, while using work-hardening plasticity models applied to the soil – foundation system, can lead to a more appropriate representations of the yield surface, which can in turn produce a more precise estimates of the complete load-displacement response of the foundation, predicting accurately the yielding threshold from which combined plastic displacements are calculated.

It is, however, worth to observe that the results might not be adequate to represent the foundation behaviour outside the investigated range.

At low values of vertical load and thus at low values of vertical penetration (w/B < 0.1), variations in the sand dilation and permanent deformations, mobilised prior to yield can play a major role on the soil-foundation combined loading response, which the simple model used in this study, is not suitable to capture. To explore these aspects more comprehensively a less schematic constitutive model is needed, which can incorporate strain-dependent dilatancy and hardening features. However, the description of the yield surface close to the load axis origin is relevant to very specific applications, such as, for instance, caisson foundations for wind turbines.

As it was observed by the results of swipe tests carried out on the most embedded foundation (d/B = 1), the yield surface is shown to slightly deviate from the traditional cigar-shape described by Eq. (1). Therefore further investigation are needed to explore the yield surface features for higher depth ratios (d/B > 1), as the traditional approach may no longer hold.

Finally, further analyses may consider in more details the shape effects on the yield surface, to provide confidence in applying results obtained in plane-strain conditions to three-dimensional problems.

5. Concluding remarks

Within the context of work-hardening plasticity models of the soil-foundation system, the paper has presented a numerical study of the embedment effects on the yield surface for a shallow foundation in sand. The numerical approach was validated based on data from centrifuge tests available in literature, across a practical range of foundation initial depth, d, mobilised vertical load, V_0, and combined load paths. The comparison has proved the model able in reproducing the experimentally observed foundation response to combined loading. The study has shown that, for a shallow foundation embedded in sand:

- the yield surface which is established in the load space is essentially parabolic in planes containing the V axis, with elliptical, anticlockwise rotated, sections with planes at constant V;
- existing equations of the yield surface for the soil-foundation system still work well, but modifications need to be introduced to account of effects of the embedment, which are not negligible;
- the extent and rotation of the normalised yield surface are function of the embedment as produced by the coupled effect of the foundation initial depth, d, and mobilised penetration, w.

Therefore, simple algebraic expressions were proposed to:

- approximate the yield surface for selected values of foundation initial depth, d, and vertical penetration, w, as produced by a known uniaxial vertical load, V;
- provide an accurate yielding threshold to work-hardening plasticity models for the prediction of the combined plastic displacements of an embedded foundation.

Overall, the results of the study also offers a convenient starting point to the development of complete work-hardening plasticity models of the soil-foundation system for embedded foundations. This would encourage the application of these approaches, whose use is now a well-established practice in the offshore environment, to onshore foundations, typically buried at some depth below the ground level.

Acknowledgements

Luigino Albanesi, Martina Grimandi and Manuel Pratelli, former master students at the University of Bologna, Italy, are sincerely acknowledged for their contribution to this work. Professor Susan Gourvenec is also acknowledged for the support given in the FE modelling of the centrifuge tests.

References

[1] Butterfield R, Ticof J. Design parameters for granular soils (discussion contribution). In: Proc. 7th European conf. soil mech. and foundation engng (ECSMFE), Brighton, vol. 4. p. 259–61.
[2] Nova R, Montrasio L. Settlements of shallow foundations on sand. Geotechnique 1991;2:243–56.
[3] Houlsby GT, Cassidy MJ. A plasticity model for the behaviour of footing on sand under combined loading. Géotechnique 2002;2:117–29.
[4] Gottardi G, Houlsby GT, Butterfield R. Plastic response of circular footings on sand under general planar loading. Géotechnique 1999;4:453–69.

Please cite this article in press as: Govoni L. A numerical investigation on the yield surface for shallow foundations embedded in sand. Comput Geotech (2017), http://dx.doi.org/10.1016/j.compgeo.2017.08.017

[5] Bienen B, Byrne BW, Houlsby GT, Cassidy MJ. Investigating six-degree-of-freedom loading of shallow foundations on sand. Geotechnique 2006;6:367–79.
[6] Cassidy MJ. Experimental observations of the combined loading behaviour of circular footings on loose silica sand. Géotechnique 2007;4:397–401.
[7] Byrne BW, Houlsby GT. Observation of footing behaviour on loose carbonate sand. Geotechnique 2001;5:463–6.
[8] Govoni L, Gourvenec S, Gottardi G. Centrifuge modelling of circular shallow foundations on sand. Int J Phys Modell Geotech 2010;2:35–46.
[9] Montrasio L, Nova R. Settlements of shallow foundations on sand: geometrical effects. Géotechnique 1997;1:49–60.
[10] Byrne BW, Houlsby GT. Drained behaviour of suction caisson foundations on very dense sand. In: Proc. Offshore Technology Conf., Houston, TX, Paper 10994; 1999.
[11] Villalobos FA, Byrne BW, Houlsby GT. An experimental study of the drained capacity of suction caisson foundations under monotonic loading for offshore applications. Soils Found 2009;3:477–88.
[12] Foglia A, Gottardi G, Govoni L, Ibsen LB. Modelling the drained response of bucket foundations for offshore wind turbines under general monotonic and cyclic loading. Appl Ocean Res 2015;52:80–91.
[13] Govoni L, Gourvenec S, Gottardi G. A centrifuge study on the effect of embedment on the drained response of shallow foundations under combined loading. Géotechnique 2011;12:1055–68.
[14] Bransby MF, Randolph MF. Combined loading of skirted foundations. Géotechnique 1998;5:637–55.
[15] Bienen B, Gaudin C, Cassidy MJ, Rausch L, Purwana OA, Krisdani H. Numerical modelling of a hybrid skirted foundation under combined loading. Comput Geotech 2012;45:127–39.
[16] Karapiperis K, Gerolymos N. Combined loading of caisson foundations in cohesive soil: finite element versus Winkler. Comput Geotech 2014;56:100–20.
[17] Shen Z, Feng S, Gourvenec S. Undrained capacity of surface foundations with zero-tension interface under planar V-H-M loading. Comput Geotech 2016;73:47–57.
[18] Achmus M, Akdag CT, Thieken K. Load-bearing behavior of suction bucket foundations in sand. Appl Ocean Res 2013;10:157–65.
[19] Zafeirakos A, Gerolymos N. Bearing strength surface for bridge caisson foundations in frictional soil under combined loading. Acta Geotech 2016;11:1189–208.
[20] Gottardi G, Govoni L, Butterfield R. Yield loci for shallow foundations by 'swipe' testing. In: Proceedings of the 1st International Symposium on Frontiers in Offshore Geotechnics; 2005. p. 469–75.
[21] Krabbenhoft S, Damkilde L, Krabbenhoft K. Bearing capacity of strip footings in cohesionless soil subject to eccentric and inclined loads. Int J Geomech 2014;3:04014003.
[22] Yahia-Cherif H, Mabrouki M, Benmeddour D, Mellas M. Bearing capacity of embedded strip footings. Geotech Geol Eng 2017;35:547–58.
[23] Gourvenec S, Govoni L, Gottardi G. An investigation of shallow foundations on sand under moment loading. In: Proc. 2nd BGA Int. Conf. on Foundations 2008; 2008. p. 873–84.
[24] Butterfield R. On shallow pad-foundations for four-legged platforms. Soils Found 2006;4:427–35.
[25] Butterfield R. On dimensioning the base of a traditional retaining wall. Geotech Lett 2012;4–6:25–8.
[26] Marchi M, Butterfield R, Gottardi G, Lancellotta R. Stability and strength analysis of leaning towers. Geotechnique 2011;12:1069–79.
[27] Butterfield R, Gottardi G, Houlsby GT. Standardised sign conventions and notation for generally loaded foundations. Geotechnique 1997;4:1051–2.
[28] Dassault Systemes. Abaqus analysis user's manual. Providence, RI: Simulia Corp; 2012.
[29] Martin CM. ABC - Analysis of Bearing Capacity, Version 1.0, User Guide, Report OUEL No. 2261/03; 2003.

Please cite this article in press as: Govoni L. A numerical investigation on the yield surface for shallow foundations embedded in sand. Comput Geotech (2017), http://dx.doi.org/10.1016/j.compgeo.2017.08.017